Large-Area MEMS Tunable Fabry–Perot Filters for Multi/Hyperspectral Infrared Imaging

Haifeng Mao, Dhirendra Kumar Tripathi, *Member, IEEE*, Yongling Ren, K. K. M. B. Dilusha Silva, *Member, IEEE*, Mariusz Martyniuk, *Member, IEEE*, Jarek Antoszewski, John Bumgarner, John M. Dell, *Member, IEEE*, and Lorenzo Faraone, *Fellow, IEEE*

***Abstract*—This paper reports on a MEMS tunable Fabry–Perot filter technology capable of achieving nanometer-scale optical flatness across a large mirror area of up to square centimeters without any extraneous stress management techniques. The device employs a single-layer tensile silicon or germanium membrane for the suspended top mirror. Optical characterization of the fabricated single-membrane-based tunable filters for the SWIR, MWIR, and LWIR is presented. The fabricated 1000-μm dimension Si-membrane-based SWIR and MWIR filters are demonstrated with a wavelength tuning range of 1.77–2.42 and 4.1–4.9 μm, respectively, while the fabricated 200-μm-dimension Ge-membrane-based LWIR filter is demonstrated with a wavelength tuning range of 8.5–11.46 μm. All these filters are shown to achieve transmission characteristics that exceed the optical requirements for multispectral imaging applications. A large-area 1-cm dimension Si membrane-based SWIR tunable Fabry–Perot filter for multispectral imaging is demonstrated as a proof-of-concept, showing an excellent surface flatness in the order of 25 nm and an excellent optical uniformity with transmission peak wavelength variability less than 3% across the entire 1-cm dimension optical imaging area. In addition, the optical transmission behavior of the Fabry–Perot filters based on three-layer Si or Ge-based air-spaced DBRs for SWIR, MWIR, and LWIR is modeled, demonstrating that these filters can achieve a fine spectral resolution of several tens of nanometers suitable for hyperspectral imaging applications.**

***Index Terms*—Fabry-Perot interferometers, hyperspectral/multispectral infrared imaging, MEMS.**

I. Introduction

CURRENT state-of-the-art infrared imaging technologies incorporate so-called multi/hyper-spectral capabilities, which allow real-time spectral information to be gathered from multiple wavelength bands. Multi/hyper-spectral imaging systems can extract spectral signatures of objects, and thus provide enhanced detection and discrimination of targets in clutter in comparison to single-band imaging systems. A common criterion to distinguish hyperspectral imaging from multispectral imaging is the number of spectral channels. While most hyperspectral imaging systems collect 100 or more contiguous spectral bands, multispectral imaging systems typically acquire less than 20, non-contiguous spectral bands [1], [2], although there is no consensus on exact values. The utility of multi/hyper-spectral imaging systems has been well established in the domain of the SWIR (short-wavelength infrared, 1.6–2.5 μm), MWIR (mid-wavelength infrared, 3–5 μm), and LWIR (long-wavelength infrared, 8–12 μm) for a wide variety of applications, such as gas and volatile organic compound diagnostics [3]–[5], mineral mapping [6], [7], and global atmospheric temperature profile monitoring [8], [9]. According to [3]–[9], it can be inferred that hyperspectral imaging systems typically collect spectral bands of very narrow spectral width ($\delta\lambda/\lambda_c < 1\%$, $\delta\lambda$: full-width at half-maximum, λ_c: central wavelength) and have a very wide capability of spectral discrimination, whereas multispectral imaging systems collect spectral bands of relatively broad bandwidth ($\delta\lambda/\lambda_c \sim 5\%$), and are designed to support applications by providing bands that detect information in specific combinations of desirable regions of the spectrum. In conventional multispectral imaging systems, spectral selection is typically implemented by means of a series of band-pass interference filters mounted on a motorized wheel, while in conventional hyperspectral imaging systems, the spectral selection function is realized using dispersive grating/prism or optical interferometers [1]. These types of configuration, based on standard bulk optics, are characterized by significant size, weight and power (SWaP), which prohibit their widespread use in many desirable applications requiring field portability or mounting on UAV platforms. In order to provide a more robust filter solution with reduced SWaP, a microelectromechanical systems (MEMS) based electrically tunable Fabry-Perot filter technology is proposed.

A MEMS-based Fabry-Perot filter consists of a top movable mirror suspended over a bottom fixed mirror, forming an optical cavity. The mirrors are typically distributed Bragg reflectors (DBRs) composed of alternating quarter-wavelength thick layers of high-refractive-index and low-refractive-index materials. Ideally, the optical transmission peak of the filter occurs at

Manuscript received June 7, 2016; revised September 26, 2016 and November 26, 2016; accepted December 20, 2016. Date of publication December 22, 2016; date of current version March 8, 2017. This work was supported in part by the Australian Research Council, in part by the Office of Science of the Western Australian State Government, in part by the Western Australian Node of the Australian National Fabrication Facility, a company established under the National Collaborative Research Infrastructure Strategy to provide nano and microfabrication facilities for Australian researchers.

H. Mao, D. K. Tripathi, Y. Ren, K. K. M. B. D. Silva, M. Martyniuk, J. Antoszewski, J. M. Dell, and L. Faraone are with the School of Electrical, Electronic and Computer Engineering, University of Western Australia, Crawley, WA 6009, Australia (e-mail: haifeng.mao@uwa.edu.au; dhirendra.tripathi@research.uwa.edu.au; yongling.ren@uwa.edu.au; dilusha.silva@uwa.edu.au; mariusz.martyniuk@uwa.edu.au; jarek.antoszewski@uwa.edu.au; john.dell@uwa.edu.au; lorenzo.faraone@uwa.edu.au).

J. Bumgarner is with the Panorama Synergy, West Perth, WA 6005, Australia (e-mail: jbumgarner@panoramasynergy.com).

Color versions of one or more of the figures in this paper are available online at http://ieeexplore.ieee.org.

Digital Object Identifier 10.1109/JSTQE.2016.2643782

TABLE I
SPECTRAL SPECIFICATIONS OF TUNABLE FABRY-PEROT FILTERS FOR SWIR, MWIR AND LWIR MULTISPECTRAL AND HYPERSPECTRAL IMAGING

Parameter	Multispectral imaging			Hyperspectral imaging			Comment
	SWIR (1.6–2.5 μm)	MWIR (3–5 μm)	LWIR (8–12 μm)	SWIR (1.6–2.5 μm)	MWIR (3–5 μm)	LWIR (8–12 μm)	
Peak transmission	$>50\%$	$>50\%$	$>50\%$	$>50\%$	$>50\%$	$>50\%$	Optical throughput for high signal-to-noise ratio
FWHM	$\sim$150 nm	$\sim$350 nm	$\sim$500 nm	$\sim$16–25 nm	$\sim$30–50 nm	$\sim$80–120 nm	Optical throughout and wavelength discrimination
Peak wavelength variation	$<6\%$	$<6\%$	$<6\%$	$<1\%$	$<1\%$	$<1\%$	Pixel-to-pixel wavelength uniformity across a FPA

the resonant wavelength that is exactly double the optical cavity length, when operating in first-order [10]. For other wavelengths, the optical transmission falls off rapidly away from the peak value, creating a spectrally isolated transmission pass-band. Using a MEMS actuator to control the mirror separation, the transmission pass-band can be swept over a range of wavelengths, creating a tunable optical filter.

In order to achieve the desirable spectral resolution for multi/hyper-spectral imaging applications, Fabry-Perot filters require highly reflective DBRs. The reflectivity of a DBR is dependent on the refractive index contrast between the mirror materials and the number of material pairs in the DBR. The higher the material refractive index contrast and the greater the number of periods in the DBR, the higher reflectivity the DBR. Whilst MEMS-based infrared Fabry-Perot filters have been previously reported [11]–[16], they consisted of multi-layer semiconductor or dielectric based DBRs. Due to the close refractive indices of the solid materials, DBRs in these filters employed a large number of material pairs in order to achieve high reflectivity. The successful development of these filters is technologically challenging due to the stress induced bowing of suspended mirrors. These filter technologies incorporated either complicated processing steps or complex MEMS design to control the stress gradients, and only allowed fabrication of devices with relatively small optical areas, which are not suitable for hybridization with large-format infrared imaging focal plane arrays (FPAs). Milne *et al.* [11] employed a three-layer Ge/SiO/Ge top mirror and a four-layer Ge/SiO/Ge/SiO bottom mirror to realize a 70-μm diameter MEMS-based tunable SWIR filter, which achieved a continuous wavelength tuning range of 1.6–2.4 μm with a consistent FWHM of 52 nm. To eliminate top mirror bowing, a post-fabrication oxygen plasma treatment was used to balance the stress gradient in the top mirror and to correct mirror curvature. Neumann *et al.* [13] reported a 1.9 mm $\times$ 1.9 mm large-area MEMS-based tunable MWIR filter based on four-layer Si/SiO_2/Si/SiO_2 mirrors. This filter demonstrated a wavelength tuning range of 4.0–5.0 μm with a FWHM of approximately 100 nm. In Neumann's design, 300 μm thick, mechanically stiff Si wafers were used as mirror carriers and, in particular, the mirror deposition process was optimized to control top mirror bowing. Based on the same design, Ebermann *et al.* [14] developed a MEMS-based dual-band IR filter using multilayer Ge/ZnS-based mirrors, and this filter was reported to have a LWIR tuning range of 8–10.5 μm with 105–200 nm FWHM in the first interference order and simultaneously exhibit a MWIR tuning range of 3.9–4.8 μm with 55–80 nm FWHM in the second interference order. However, due to significant mass of the top movable mirror carrier, these two filters exhibited significant acceleration sensitivity. In order to overcome this challenge, Meinig *et al.* [15] from the same research group improved the design with two suspended movable mirror carriers and developed a 2 mm $\times$ 2 mm dimension MEMS-based MWIR/LWIR dual-band infrared filter. In addition, Stupar *et al.* [16] fabricated a 200-μm dimension LWIR tunable filter with 13 μm thick multilayer DBR mirrors (materials not disclosed) based on a SOI device layer transfer process, demonstrating a wavelength tuning range of 8–11 μm with a 120 nm FWHM. For this filter, the top mirror stress gradient was balanced by tailoring the mirror layer stress conditions during deposition.

In previous work, our research group developed high-refractive-index tensile Si thin film technologies for MEMS optical membrane applications [17]. Our research group also fabricated a static LWIR Fabry-Perot filter based on a high-refractive-index single Ge membrane technology [18], and further demonstrated an electrically tunable LWIR filter using a stretched-membrane MEMS structure for multispectral thermal imaging [19]. Based on the same MEMS design in [19], the present paper reports on new results for our recently developed Si single-membrane based SWIR and MWIR tunable filters as well as centimeter-scale large-area MEMS-based tunable SWIR Fabry-Perot filter technologies for multispectral infrared imaging applications. High-index Si and Ge films not only can provide sufficient reflectivity by just using a single layer, but also can combine with air to form air-spaced DBRs which, due to the very high refractive index contrast, can produce extremely high mirror reflectivity over a broad bandwidth. Another advantage of the air-spaced DBRs is that they are not subject to any film stress mismatch issues because there is no material mismatch, allowing fabrication of large-dimension filters. Tuohiniemi *et al.* [20] first realized a MEMS-based tunable LWIR filter based on two suspended Si/air/Si mirrors. This filter had a 0.8-mm diameter optical aperture and demonstrated a continuous wavelength tuning range of 7.9–11.24 μm with a FWHM of 140 nm. This paper also reports on filter design and modelling for MEMS tunable SWIR, MWIR and LWIR Fabry-Perot filter technologies based on air-spaced Si or Ge mirrors for hyperspectral imaging. Table I shows the optical performance requirements of tunable filters for multi/hyper-spectral imaging applications.

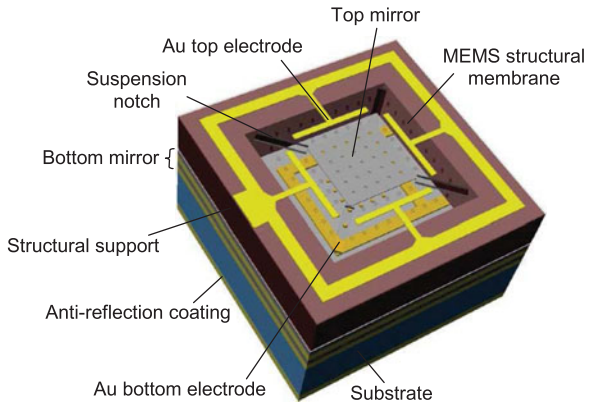

Fig. 1. Graphical depiction of the single-membrane based MEMS tunable Fabry-Perot filter. The top MEMS structural membrane is drawn semi-transparent to allow the bottom electrode layout to be visible. This MEMS schematic was first presented in [19].

II. MEMS Technologies

The proposed single-membrane based MEMS tunable Fabry-Perot filter structure is schematically shown in Fig. 1. A movable top mirror membrane is suspended over a fixed bottom mirror on a substrate, creating a tunable optical resonant cavity. A quarter-wavelength thick anti-reflection coating is deposited on the backside of the substrate to reduce backside reflections at the substrate-air interface, thus improving the optical transmission of the filter. The top mirror is located in the center of the suspended MEMS structural membrane, which extends all the way to the outer perimeter of the solid structural support. The most obvious advantage of this MEMS design is that any tensile stress inherent in the thin film will tend to stretch the whole suspended membrane, thus aiding in flattening the central mirror and eliminating the need for any stress management. Four driving electrodes are deposited on the MEMS structural membrane around the central mirror which, in combination with the underlying bottom electrode, move the top mirror closer to the bottom mirror during electrostatic actuation. Diagonally arranged notches at the corners of the structural membrane serve to release the convergence of tensile stress from two orthogonal directions, allowing freestanding membrane actuation without causing stress induced distortion in the central mirror. These notches also reduce the spring stiffness of the membrane and thus allow low-voltage actuation. An array of 5-μm diameter holes perforated in the membrane facilitates the sacrificial layer etching process. These etch holes are only included in the proof-of-concept design, and can be removed in any future development. The optical path of the etch hole array is masked by an array of Au micropatterns deposited on the bottom mirror. In addition, an Au optical shield layer with a central window matched to the mirror dimension is deposited on the backside of the substrate in order to block stray light from outside of the mirror area (not shown).

III. Single-membrane based Tunable Fabry-Perot Filters for Multispectral Imaging

Based on the MEMS design shown in Fig. 1, single-membrane based tunable Fabry-Perot filters for multispectral infrared imaging were fabricated. These filters are based on single-membrane Si or Ge top mirrors. The optical layer structures of the SWIR, MWIR and LWIR filters are given in Table II.

A. Si Membrane Based SWIR Filters

The SWIR Fabry-Perot filters for multispectral imaging consist of a single layer of Si as the top suspended mirror and a two-layer Si/SiO_x bottom mirror on a silicon substrate, with Si and SiO_x having quarter-wavelength thicknesses of 135 nm and 316 nm, respectively. Filters of 1000-μm optical mirror dimension were fabricated, and the surface profiles of the freestanding membranes of the as-released filters were measured using a non-contact optical surface profilometer. These measurements indicated that the mirrors of the fabricated filters exhibited excellent flatness, with a center-to-edge bowing magnitude of 13 nm across the entire 1000-μm dimension area.

Transmission spectra of the SWIR filters were measured as a function of actuation voltage, and the results are presented in Fig. 2(a) using data points. The solid lines in Fig. 2(a) represent the modelled optical transmission spectra, which show a strong agreement with the experimentally measured results. As can be seen in Fig. 2(a), the measured wavelength tuning range of the SWIR filter was observed to be 1.77–2.42 μm and was obtained using a maximum actuation voltage of 57 V. This wavelength tuning range accounts for 72.2% of the complete SWIR band of 1.6–2.5 μm. The filter demonstrated consistent transmission characteristics over the entire wavelength tuning range; namely, a peak transmission between 60% and 65% and a FWHM between 160 nm and 180 nm, which meet the optical requirements for multispectral SWIR imaging applications as listed in Table I.

B. Si Membrane Based MWIR Filters

The MWIR Fabry-Perot filters for multispectral imaging have the same mirror structures as the SWIR filters, consisting of a single-layer Si top mirror and a two-layer Si/SiO_x bottom mirror on a silicon substrate. The Si and SiO_x layers have the quarter-wavelength thicknesses of 264 nm and 616 nm, respectively. The as-released MWIR filters demonstrated excellent mirror flatness, with a center-to-edge bowing magnitude of 15 nm across the entire 1000-μm dimension optical mirror area.

The experimentally measured transmission spectra for the actuated MWIR filter are shown in Fig. 2(b). It can be seen from Fig. 2(b) that the optical transmission of the MWIR filter can be continuously tuned from 4.1 μm to 4.9 μm using a maximum actuation voltage of 25 V, which accounts for 40% of the complete MWIR wavelength band of 3–5 μm. The filter can achieve a peak transmission in the range of 65–75% and a FWHM of approximately 360 nm over the entire wavelength tuning range, which meet the optical requirements for multispectral MWIR imaging applications as listed in Table I.

C. Ge Membrane Based LWIR Filters

The LWIR Fabry-Perot filters for multispectral imaging are composed of a single-layer Ge top mirror and a four-layer Ge/ZnS/Ge/ZnS bottom mirror on a float-zone silicon substrate,

TABLE II
OPTICAL LAYER STRUCTURES OF THE MEMS-BASED TUNABLE SWIR, MWIR AND LWIR FABRY-PEROT FILTERS FOR MULTISPECTRAL IMAGING

	SWIR (1.6–2.5 μm)		MWIR (3–5 μm)		LWIR (8–12 μm)	
	Material	Thickness	Material	Thickness	Material	Thickness
Top mirror	Si	135 nm	Si	264 nm	Ge	625 nm
Optical cavity	Air	1250 nm	Air	2500 nm	Air	6000 nm
Bottom mirror	Si/SiO_x	135 nm/316 nm	Si/SiO_x	264 nm/616 nm	Ge/ZnS/Ge/ZnS	625 nm/1136 nm
Substrate	Silicon	300 μm	Silicon	300 μm	Float-zone silicon	300 μm
Anti-reflection coating	SiO_x	316 nm	SiO_x	616 nm	ZnS	1136 nm

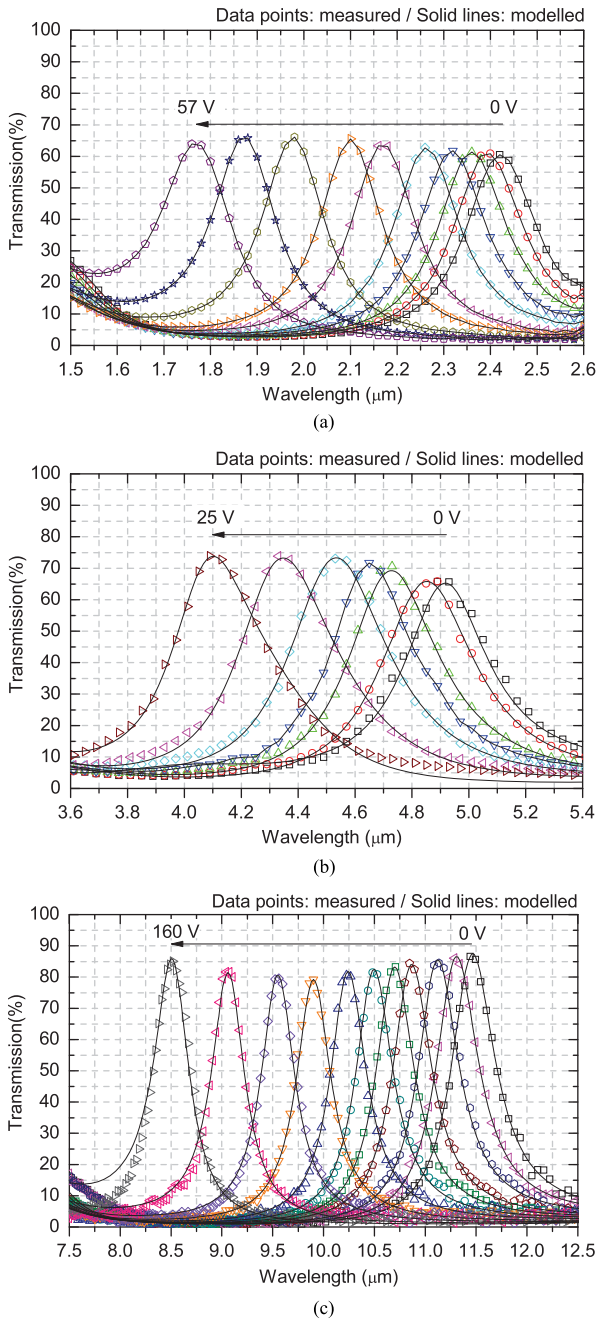

Fig. 2. Transmission tuning spectra for single-membrane based (a) SWIR, (b) MWIR and (c) LWIR Fabry-Perot filters. The data points and solid lines correspond to the measured results and the modelled results, respectively. The data in Fig. 2(c) were presented previously in [19].

where the Ge and ZnS layers have quarter-wavelength thicknesses of 625 nm and 1136 nm, respectively. Float-zone silicon substrates were used simply because it contains negligible amounts of oxygen and exhibits excellent LWIR transparency as compared to standard Czochralski silicon wafers [21]. Optical profilometry measurements showed that the mirrors of the un-actuated LWIR filters exhibited near-perfect flatness, with bowing on the nanometer scale across the entire 1000-μm dimension optical imaging area.

As can be seen in Fig. 2(c), the measured wavelength tuning range for a 200-μm dimension filter was observed to be 8.5–11.46 μm and was obtained using a maximum voltage of 160 V. This wavelength tuning range accounts for 75% of the complete thermal imaging band of 8–12 μm, and to date is the widest tuning range reported in the literature for a MEMS-based LWIR Fabry-Perot filter. The filter exhibited consistent transmission characteristics over the entire tuning range, including a high peak transmission in the range of 80–87% and a FWHM value of 400–480 nm, which exceed the optical performance requirements listed in Table I.

IV. LARGE-AREA MEMS-BASED TUNABLE FABRY-PEROT FILTERS FOR MULTISPECTRAL IMAGING

Most commercial high-definition multispectral imaging sensors make use of large-format focal plane detector arrays with a spatial resolution of 1280 × 1024. Employing such a large-format FPA, with a 15-μm pixel pitch size for example, results in the demand for a MEMS tunable filter with a large optical imaging area of approximately 2 cm × 1.5 cm. Maintaining top mirror surface flatness and parallelism to the bottom substrate is critical for successfully developing such large-dimension filters. Any suspended mirror bowing or tilt with respect to the substrate will cause a variability of the optical cavity length, which will translate into a pixel-to-pixel variation of transmission peak wavelength across the imaging focal plane array.

In this work, centimeter-scale Si-membrane based SWIR Fabry-Perot filters were fabricated for demonstrating proof-of-concept large-area filters for multispectral imaging. The surface profiles of the freestanding membranes were measured using an optical profilometer. A line scan across the 1-cm silicon membrane is shown in Fig. 3(a). As evident from Fig. 3(a), the as-released membrane exhibited near-perfect surface flatness, with a profile variation of less than 25 nm across the entire 1-cm dimension area. Fig. 3(a) also shows the measured substrate profile for comparison, and it is noteworthy to

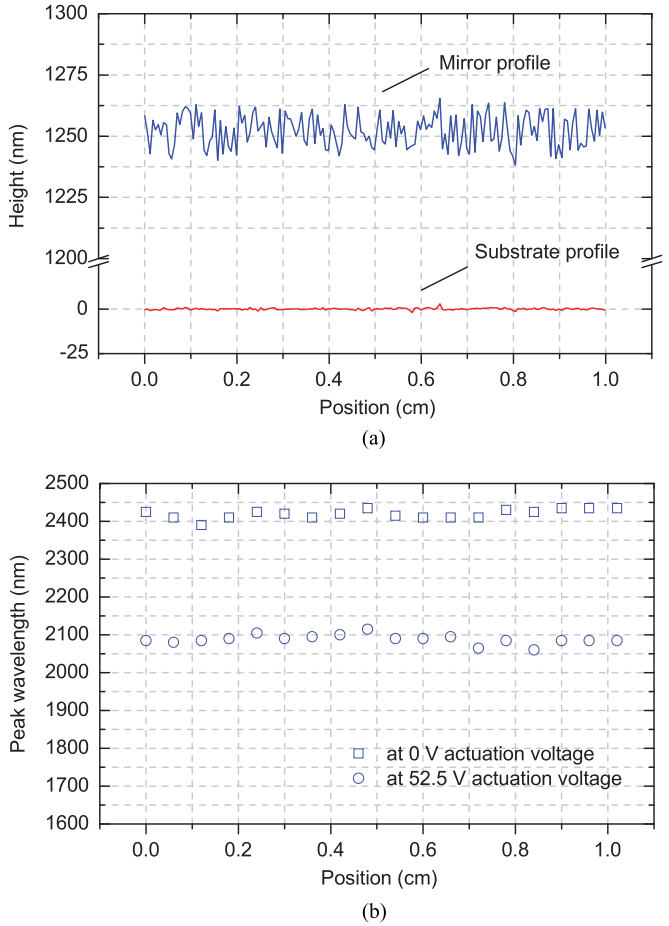

Fig. 3. (a) shows the measured mirror surface line profile across a fabricated 1-cm dimension single Si membrane based SWIR Fabry-Perot filter. (b) shows the transmission peak wavelength over a 20 μm $\times$ 20 μm pixel area at various spatial positions of the filter.

observe that the 1-cm dimension membrane exhibited negligible tilt with respect to the substrate.

The optical spatial uniformity over the 1-cm dimension optical imaging area was examined using an in-house developed optical metrology system [22]. This system enables the spatial mapping of optical transmission spectra across the filter imaging area within the spectral band from 1400 nm to 2600 nm. The light beam was focused down to a spot size of 20 μm, which is comparable to the pixel pitch size in FPAs, and the optical transmission was scanned across the 1-cm dimension optical imaging area with a step size of 500 μm. Fig. 3(b) shows the extracted central transmission peak wavelength as a function of spatial position on the filter. It can be seen in Fig. 3(b) that the un-actuated filter had a nominal transmission peak wavelength of 2.4 μm. The maximum on-pixel transmission peak wavelength was measured to be 2.44 μm, and the minimum on-pixel peak wavelength was measured to be 2.39 μm, corresponding to a pixel-to-pixel transmission peak wavelength variation of 2.1%. Using an actuation voltage of 52.5 V, the optical transmission of the filter was tuned to a nominal central wavelength of 2.1 μm. The maximum on-pixel transmission peak wavelength variation across the entire 1-cm optical imaging area was observed to be 55 nm, which corresponds to a pixel-to-pixel peak

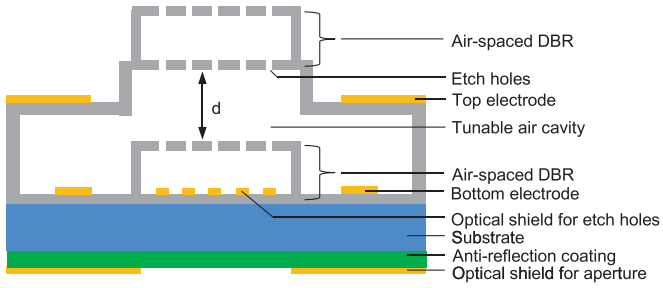

Fig. 4. Schematic cross-section of the MEMS tunable Fabry-Perot filters based on air-spaced mirrors for hyperspectral imaging.

wavelength variability of 2.6%. This excellent pixel-to-pixel peak wavelength uniformity is a direct consequence of the achieved level of suspended top mirror flatness, and exceeds the optical specifications for multispectral imaging applications as listed in Table I, demonstrating that the single-membrane MEMS-based Fabry-Perot filter shown in Fig. 1 is a feasible design for fabricating large-area tunable optical filters for hybridizing with high-definition large-format FPAs.

V. Large-area MEMS-based Tunable Fabry-Perot Filters for Hyperspectral Imaging

Based on the excellent results demonstrated for the single-membrane based large-area Fabry-Perot filters for multispectral imaging, it is believed that the MEMS technology shown in Fig. 1 can be extended to realize large-dimension MEMS-based tunable Fabry-Perot filters for hyperspectral imaging by incorporating air-spaced mirrors to achieve the narrow linewidths required for on-pixel spectroscopy. A schematic cross-section of the proposed Fabry-Perot filter for hyperspectral imaging is shown in Fig. 4. The filter consists of a suspended air-spaced top DBR and a fixed air-spaced bottom DBR on a silicon substrate. The air-spaced DBRs are either Si/air/Si for SWIR and MWIR filters or Ge/air/Ge for the LWIR filter. While the Si layers for SWIR and MWIR filters have the quarter-wavelength thicknesses of 135 nm and 264 nm, respectively, the Ge layers for LWIR filter have a quarter-wavelength thickness of 625 nm. The air-gaps in the DBRs can be realized by etching polyimide sacrificial layers through the etch holes perforated in the mirrors, with quarter-wavelength thicknesses of 500 nm, 1000 nm and 2500 nm respectively for SWIR, MWIR and LWIR filters. The bottom layer in the top suspended DBR extends outwards to serve as the MEMS structural support, on which Au electrodes are deposited for electrostatic actuation. Anti-reflection coating, that is, 316 nm SiO_x for SWIR filter, 616 nm thick SiO_x for MWIR filter, and 1136 nm thick ZnS for LWIR filter, can be deposited on the backside of the substrate to suppress the effect of multiple reflections. In addition, another Au optical shielding layer can be deposited on the backside of the substrate to define the optical aperture of the filters.

In order to investigate the suitability of three-layer air-spaced DBRs for fabricating tunable Fabry-Perot filters for hyperspectral imaging applications, the optical transmission of the filter shown in Fig. 4 was modelled for various optical cavity lengths for SWIR, MWIR and LWIR cases, and the results are shown in

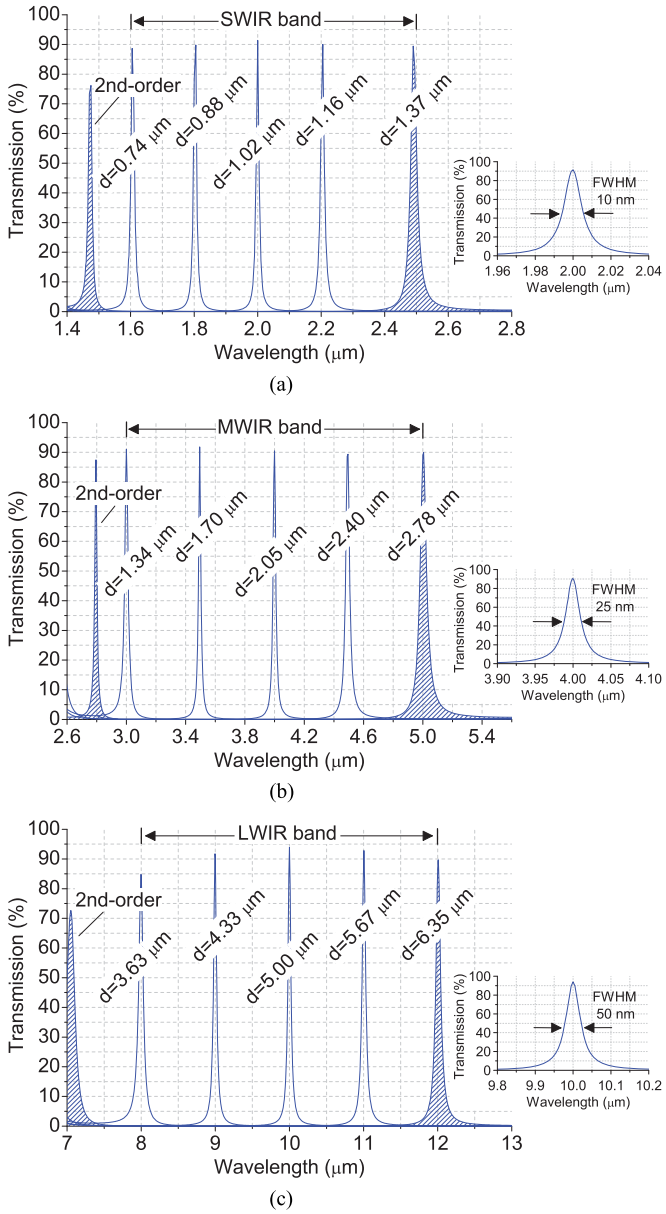

Fig. 5. The modelled optical transmission of the Fabry-Perot filters based on air-spaced DBRs for various optical cavity lengths. (a), (b) and (c) show the results for SWIR filter, MWIR filter and LWIR filter, respectively.

Fig. 5. As can be seen in Fig. 5(a), the SWIR filter is predicted to have a high peak transmission of 90% and a narrow FWHM of 10 nm across the entire SWIR range of 1.6–2.5 μm when the optical cavity is tuned from 1.37 μm to 0.74 μm. Fig. 5(b) shows that a peak transmission greater than 90% and a narrow FWHM of 25 nm can be achieved for the Si/air/Si DBR based MWIR filter over the entire MWIR range of 3–5 μm. As evident from Fig. 5(c), a LWIR filter based on Ge/air/Ge DBRs is predicted to exhibit consistent transmission characteristics over the entire LWIR range of 8–12 μm, including a peak transmission greater than 85% and a narrow FWHM of 50 nm. All these spectral figures exceed the optical specifications as listed in Table I, indicating that high spectral resolution MEMS-based tunable Fabry-Perot filters for hyperspectral infrared imaging can be readily realized using three-layer air-spaced DBRs.

VI. Conclusions

This paper has reported the realization of a MEMS-based tunable Fabry-Perot filter technology, employing a single-layer tensile-strained Si or Ge membrane as the suspended top mirror that requires no additional stress management to achieve excellent as-released mirror flatness over a large optical mirror area of centimeter dimension. The fabricated Si membrane based tunable SWIR filter of 1000 μm in dimension demonstrated a continuous wavelength tuning range of 1.77–2.42 μm with a peak transmission of 60–65% and a FWHM of 160–180 nm, while the 1000-μm dimension Si membrane based MWIR filter demonstrated a wavelength tuning range of 4.1–4.9 μm with a peak transmission in the range of 65–75% and a FWHM of approximately 360 nm. The Ge membrane based tunable LWIR Fabry-Perot filter of 200-μm mirror dimension exhibited a peak transmission higher than 80% and a FWHM between 400–480 nm over the entire wavelength tuning range of 8.5–11.46 μm. All the achieved spectral performance parameters meet the required specifications for multispectral infrared imaging applications. Moreover, a proof-of-concept large-area single Si membrane based SWIR Fabry-Perot filter with a 1-cm dimension optical area was demonstrated, which exhibited excellent surface flatness with a measured profile variation of less than 25 nm across the entire 1 cm $\times$ 1 cm dimension optical mirror area. It has also been shown that this 1-cm dimension SWIR filter can achieve excellent pixel-to-pixel transmission peak wavelength uniformity of less than 3% during actuation. Extending the current MEMS approach towards the fabrication of tunable Fabry-Perot filters for narrow-band hyperspectral imaging is the focus of future work. To this end, optical transmission of the Fabry-Perot filters based on three-layer air-spaced DBRs was examined. Optical modelling indicates that the air-spaced DBR based SWIR, MWIR and LWIR filters have a high peak transmission of approximately 90%, with a narrow spectral resolution of 10 nm, 25 nm and 50 nm, respectively, which exceed the optical requirements for hyperspectral imaging applications. Overall, we anticipate the work presented in this paper presents important research results that can be built-upon for the future technological development of field-portable and UAV-compatible low-cost multispectral and hyperspectral imaging systems based on a hybridized technology incorporating a large-area MEMS-based tunable Fabry-Perot filter and a large-format 2-D infrared imaging focal plane array.

References

[1] F. Vagni, "Survey of hyperspectral and multispectral imaging technologies," RTO NATO, Neuilly, France, Tech. Rep. TR-SET-065-P3, May 2007.

[2] M. Govender, K. Chetty, and H. Bulcock, "A review of hyperspectral remote sensing and its application in vegetation and water resource studies," *Water SA*, vol. 33, no. 2, pp. 145–152, Apr. 2007.

[3] L. Zhang and G. W. Small, "Automated detection of chemical vapors by pattern recognition analysis of passive multispectral infrared remote sensing imaging data," *Appl. Spectrosc.*, vol. 56, no. 8, pp. 1082–1093, Feb. 2002.

[4] S. Teggi, M. P. Bogliolo, M. F. Buongiorno, S. Pugnaghi, and A. Sterni, "Evaluation of SiO_2 emission from Mount Etna using diurnal and nocturnal multispectral IR and visible imaging spectrometer thermal IR remote sensing images and radiative transfer models," *J. Geophys. Res., Sol. Ea.*, vol. 104, no. B9, pp. 20069–20079, Sep. 1999.

[5] M. J. Wabomba, Y. Sulub, and G. W. Small, "Remote detection of volatile organic compounds by passive multispectral infrared imaging measurements," *Appl. Spectrosc.*, vol. 61, no. 4, pp. 349–358, Apr. 2007.
[6] A. B. Kahle and A. F. H. Goetz, "Mineralogic information from a new airborne thermal infrared multispectral scanner," *Science*, vol. 222, no. 4619, pp. 24–27, Oct. 1983.
[7] R. G. Vaughan, S. J. Hook, W. M. Calvin, and J. V. Taranik, "Surface mineral mapping at Steamboat Springs, Nevada, USA, with multi-wavelength thermal infrared images," *Remote Sens. Environ.*, vol. 99, no. 1/2, pp. 140–158, Nov. 2005.
[8] W. B. Clodius, C. Borel, L. Balick, and S. J. Hook, "Validation of the MTI water surface temperature retrieval algorithms," in *Proc. IEEE Int. Geosci. Remote Sens. Symp.*, 2002, pp. 30–32.
[9] A. P. Rodger, L. K. Balick, and W. B. Clodius, "The performance of the multispectral thermal imager (MTI) surface temperature retrieval algorithm at three sites," *IEEE Trans. Geosci. Remote Sens.*, vol. 43, no. 3, pp. 658–665, Mar. 2005.
[10] H. A. Macleod, "Multilayer high-reflectance coatings," in *Thin-film Optical Filters*, W. T. Welford, Ed., 3rd ed. Bristol, PA, USA: IPP, 2001, ch. 5, sec. 1, pp. 179–183.
[11] J. S. Milne, J. M. Dell, A. J. Keating, and L. Faraone, "Widely tunable MEMS-based Fabry–Perot filter," *J. Microelectromech. Syst.*, vol. 18, no. 4, pp. 905–913, Aug. 2009.
[12] A. J. Keating *et al.*, "Design and characterization of Fabry–Perot MEMS-based short-wave infrared microspectrometers," *J. Electron. Mater.*, vol. 37, no. 12, pp. 1811–1820, Aug. 2008.
[13] N. Neumann, M. Ebermann, K. Hiller, and S. Kurth, "Tunable infrared detector with integrated micromachined Fabry–Perot filter," in *Proc. SPIE*, vol. 6466, pp. 646606–646617, Jan. 2007.
[14] M. Ebermann *et al.*, "Tiny mid- and long-wave infrared spectrometer module with a MEMS dual-band Fabry–Perot filter," in *Proc. Sensor+Test Conf.: IRS*^{2}, Nürnberg, Germany, 2011, pp. 94–99.
[15] M. Meinig *et al.*, "Dual-band MEMS Fabry–Perot filter with two movable reflectors for mid- and long-wave infrared microspectrometers," in *Proc. IEEE 16th Int. Conf. Solid-State Sens., Actuators, Microsyst.*, Beijing, China, 2011, pp. 2538–2541.
[16] P. A. Stupar, R. L. Borwick, J. F. DeNatale, P. H. Kobrin, and W. J. Gunning, "MEMS tunable Fabry-Perot filters with thick, two sided optical coatings," in *Proc. IEEE 15th Int. Conf. Solid-State Sens., Actuators, Microsyst.*, Denver, CO, USA, 2009, pp. 1357–1360.
[17] D. K. Tripathi *et al.*, "Optimization of ICPCVD amorphous silicon for optical MEMS applications," *J. Microelectromech. Syst.*, vol. 24, no. 6, pp. 1998–2007, Dec. 2015.
[18] H. Mao *et al.*, "Ge/ZnS-based micromachined Fabry–Perot filters for optical MEMS in the longwave infrared," *J. Microelectromech. Syst.*, vol. 24, no. 6, pp. 2109–2116, Dec. 2015.
[19] H. Mao *et al.*, "MEMS-based tunable Fabry–Perot filters for adaptive multispectral thermal imaging," *J. Microelectromech. Syst.*, vol. 25, no. 1, pp. 227–235, Feb. 2016.
[20] M. Tuohiniemi, M. Blomberg, A. Akujarvi, J. Antila, and H. Saari, "Optical transmission performance of a surface-micromachined Fabry-Perot interferometer for thermal infrared," *J. Micromech. Microeng.*, vol. 22, no. 11, pp. 1–7, Sep. 2012.
[21] W. S. Lau, "The measurement of oxygen and carbon and other impurities in silicon," in *Infrared Characterization for Microelectronics*. Singapore: World Scientific, 1999, ch. 3, pp. 25–30.
[22] R. Rafiei *et al.*, "A versatile instrumentation system for MEMS-based device optical characterization," in *Proc. SPIE*, vol. 8923, pp. 89232V:1–89232V:9, Dec. 2013.

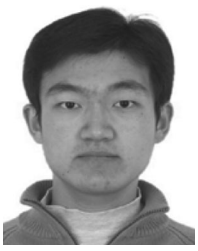

Haifeng Mao received the B.Eng. degree in physics from Dalian University of Technology, Liaoning, China, in 2007, and the M.Sc. degree in sensor systems technology from Karlsruhe University of Applied Sciences, Germany, in 2010. He was working toward the Ph.D. degree at the School of Electrical, Electronic and Computer Engineering, University of Western Australia, Perth, Australia, between 2011 and 2016. He is currently a Research Associate at the University of Western Australia. His research activities involve design, fabrication, and characterization of optical MEMS filters for multispectral imaging applications.

Dhirendra Kumar Tripathi received the B.Tech. degree in electronics engineering from Uttar Pradesh Technical University, Lucknow, India, in 2005, and the M.Tech. degree in VLSI systems from the National Institute of Technology, Tiruchirappalli, Trichy, India, in 2008. He was working toward the Ph.D. degree with the School of Electrical, Electronic and Computer Engineering, The University of Western Australia, Perth, Australia, between 2012 and 2016. He is currently a Postdoctoral Researcher at the University of Western Australia. His research activities involve design and fabrication of optical MEMS devices and materials for the MEMS.

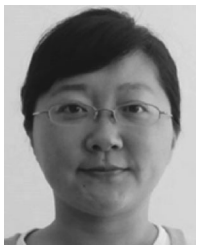

Yongling Ren received the Ph.D. degree from the Australian National University (ANU), Canberra, Australia, in 2011.

After Ph.D., she worked as a Research Fellow at ANU from 2011 to 2013, where she was involved in studies on silicon solar cells. She joined the School of Electrical, Electronic and Computer Engineering, University of Western Australia (UWA) as an Assistant Professor in 2013. Since her arrival at UWA, her research interests have been in research and development of micro-electro-mechanical systems devices.

K. K. M. B. Dilusha Silva received the Honours degrees in physics and electronic engineering from the University of Western Australia (UWA), WA, Australia, and the Ph.D. degree in optical imaging technologies for biomedical applications in 2004.

He has worked both in industry and academia, and is currently a Research Professor and the Engineering Manager with the Microelectronics Research Group, UWA. Since returning to UWA in 2009, his research interests include optical MEMS sensors, optical spectroscopic sensors, and MEMS biosensors. He has attracted funding for his research from the agriculture and aerospace sectors, and the government, and is presently leading a number of MEMS related research efforts at MRG, with strong commercial links to both the agricultural and aerospace sectors.

Mariusz Martyniuk received the B.Sc. (Hons.) degree from the University of Toronto, ON, Canada, the M.A.Sc. degree from McMaster University, ON, Canada, and the Ph.D. degree from the University of Western Australia, Perth, Australia, in 2007.

He worked in the industry sector as an Electronics Engineer before rejoining UWA, where he is currently a Research Professor with the Microelectronics Research Group and manages the Western Australian Node of the Australian National Fabrication Facility. His primary areas of interest encompass thin-film materials and thin-film mechanics, as well as their applications in micro-electromechanical systems and optoelectronic devices.

Dr. Martyniuks research contributions were recognized by the award of the Inaugural Australian Museum Eureka Prize (the Oscars of Australian science) for Outstanding Science in Support of Defence or National Security in 2008.

Jarek Antoszewski received the Master degree in physics from Teachers College in Olsztyn, Olsztyn, Poland, in 1977, and the Ph.D. degree in semiconductor physics from the Institute of Physics of Polish Academy of Science, Warsaw, Poland, in 1982.

From 1982 to 1990, he was a Researcher and then a Project Leader with the Research and Development Laboratory, WILMER Ltd., Warsaw, where he was involved in design and testing of infrared radiometers for industrial applications. In 1991, he joined the Microelectronics Research Group, University of Western Australia, Perth, WA, Australia, where he has been engaged in magnetotransport studies of semiconductor materials, and physics and technology of infrared detectors. His current research interests include the development of technology merging II–VI and III–V based infrared detectors with microelectromechanical systems technology into a new technology for monolithic and tunable infrared sensors.

John Bumgarner received the B.S. and M.S. degrees in materials science and engineering from Northwestern University, and the Ph.D. degree in materials science and engineering from North Carolina State University with a focus on wide band gap materials, SiC, and CVD of dielectrics in 1995.

He was a Process Integration Engineer and the Manager with Intel Corporation, a Laboratory Director with SRI International, and the Operations Director with Stanford University NanoFab. In 2013, he joined the Microelectronics Research Group, University of Western Australia, as an Associate Research Professor, where he has been engaged in research and development of optical microelectromechanical systems devices. Since 2016, he has been a Chief Technology Officer at Panorama Synergy, Perth, Australia, and leading the Companys MEMS sensors research and development program.

John M. Dell is currently a Professor of electrical engineering with the University of Western Australia, Perth, WA, Australia.

His primary areas of interest are semiconductor optoelectronics and optical microelectromechanical systems (MEMS) devices. He has worked in both industry and academia in these fields. Work undertaken by his group on robust and low-cost microspectrometer technology has attracted funding from the US and the Australian Department of Defence, and more recently from the Australian Grains Research and Development Corporation. This latter funding is for the development of low-cost tools using infrared spectroscopy for broad acre agriculture applications. This work is being undertaken as a collaboration between Electrical Engineers and Soil Scientists. He has several patents, and more than 200 journal and conference publications.

Lorenzo Faraone (M'79–SM'03–F'15–LF'17) received the Ph.D. degree from the University of Western Australia (UWA), Perth, WA, Australia, in 1979.

He was a Research Scientist with Lehigh University, Bethlehem, PA, USA, from 1979 to 1980, where he was involved in studies on MOS devices. From 1980 to 1986, he was a Member of the Technical Staff with RCA Laboratories, David Sarnoff Research Center, Princeton, NJ, USA, where he was involved in very large scale integration CMOS and nonvolatile memory technologies, and space radiation effects in silicon-on-sapphire MOS integrated circuits. He joined the School of Electrical, Electronic and Computer Engineering, UWA, in 1987, where he has been a Professor since 1998, and the Head of the Department/School from 1999 to 2003. Since joining UWA, his research interests have been in the areas of compound semiconductor materials and devices, and microelectromechanical systems. He has supervised more than 30 Ph.D. student completions, and published more than 300 refereed technical papers in journals and conference proceedings.

Prof. Faraone received the RCA Laboratories Individual Outstanding Achievement Award in 1983 and 1986, and the John de Laeter Innovation Award in 1997. He is a Member of the Order of Australia, and a Fellow of both the Australian Academy of Science and the Australian Academy of Technological Sciences and Engineering.